PROCEEDINGS OF SCIENCE

The rp-Process in Core-collapse Supernovae

Shinya Wanajo*
Department of Astronomy, School of Science, University of Tokyo, Bunkyo-ku, Tokyo, 113-8654
E-mail: wanajo@astron.s.u-tokyo.ac.jp

Recent hydrodynamic simulations of core-collapse supernovae with accurate neutrino transport suggest that the bulk of the neutrino-heated ejecta is proton rich, in which the production of some interesting proton-rich nuclei is expected. However, there are a number of waiting point nuclei with the β^+-lives of a few minutes, which prevent the production of heavy proton-rich nuclei beyond iron in explosive events such as core-collapse supernovae. In this study, it is shown that the rapid proton-capture (*rp*) process takes place by bypassing these waiting points via neutron-capture reactions even in the proton-rich environment, if there is an intense neutrino flux as expected during the early phase of the neutrino-driven winds of core-collapse supernovae. The nucleosynthesis calculations imply that the neutrino-driven winds can be potentially the origin of light *p*-nuclei including ^{92,94}Mo and ^{96,98}Ru, which cannot be explained by other astrophysical sites.

International Symposium on Nuclear Astrophysics — Nuclei in the Cosmos — IX
June 25-30 2006
CERN, Geneva, Switzerland

*Speaker.

PoS(NIC-IX)190

1. INTRODUCTION

The rapid proton-capture (*rp*) process has been expected to take place in proton-rich compositions with sufficiently high temperature [1] such as in X-ray bursts [2], whose nucleosynthetic products might contribute to the Galactic chemical evolution of some proton-rich isotopes including *p*-nuclei. Recent hydrodynamic simulations of core-collapse supernovae with accurate neutrino transport show that the bulk of the neutrino-heated ejecta during the early phase is proton rich [3], in which the production of some proton-rich nuclei is expected. In such environments, the waiting point nuclei (e.g., ^{64}Ge) are bypassed via neutron capture reactions even in proton-rich matter, as first pointed out by [5] (νp-process). As a result, the *rp*-process-like nucleosynthesis takes place that leads to the production of proton-rich nuclei beyond $A \sim 100$ [4, 6]. A more detailed discussion of the current results is presented in [6].

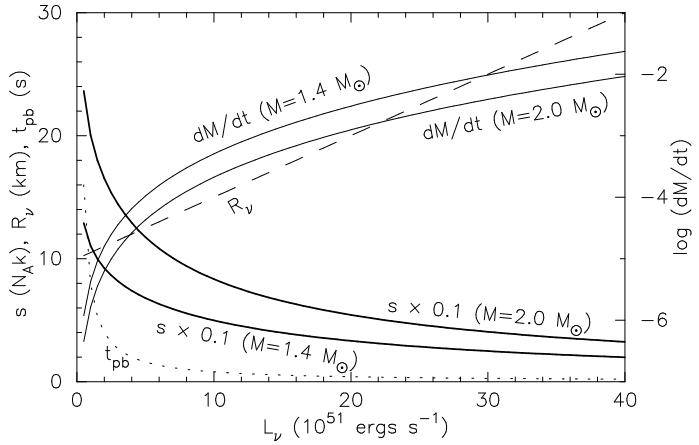

Figure 1: Model parameters ($R_\nu, t_{\rm pb}, \dot{M}$) are shown as functions of L_ν. Also denoted are the obtained entropies for $1.4M_\odot$ and $2.0M_\odot$ cases.

2. NEUTRINO-DRIVEN WINDS

Assuming the spherical symmetry of the neutrino-driven winds from a nascent neutron star, the equations of baryon, momentum, and mass-energy conservation with the Schwarzschild metric can be solved numerically [7, 8, 9]. Once the neutron star mass (M), the neutrino sphere radius (R_ν), and the neutrino luminosity (L_ν, of one flavor, where each flavor is assumed to have the same luminosity) are specified along with the mass ejection rate ($\dot{M}$) as the boundary condition, the wind solution can be obtained. In this study, the neutron star mass is taken to be $1.4M_\odot$ and $2.0M_\odot$.

The time evolutions of L_ν and R_ν are assumed to be $L_\nu(t_{\rm pb}) = L_{\nu 0}(t_{\rm pb}/t_0)^{-1}$ and $R_\nu(t_{\rm pb}) = (R_{\nu 0} - R_{\nu f})(t_{\rm pb}/t_0)^{-1} + R_{\nu f}$, where $t_{\rm pb}$ is the post-bounce time, $t_0 = 0.2$ s, $L_{\nu 0} = 4 \times 10^{52}$ ergs s^{-1}, $R_{\nu 0} = 30$ km, and $R_{\nu f} = 10$ km, which mimic the hydrodynamic results of the neutrino-driven winds in [10]. The wind trajectories are calculated for 54 constant L_ν between 0.5 and 40 ergs s^{-1}. Figure 1 shows the obtained entropies in winds for $1.4M_\odot$ and $2.0M_\odot$ cases as functions of L_ν, along with the morel parameters $\dot{M}$, R_ν, and $t_{\rm pb}$.

3. NUCLEOSYNTHESIS

The nucleosynthetic yields for each wind trajectory are obtained by application of an extensive nuclear reaction network that consists of ~ 6300 species between the proton and neutron drip lines along with all relevant nuclear reaction and weak rates [11]. The neutrino captures on free nucleons are also included. Each calculation is initiated ($t = 0$ s) when the temperature decreases to $T_9 = 9$ (where $T_9 \equiv T/10^9$ K).

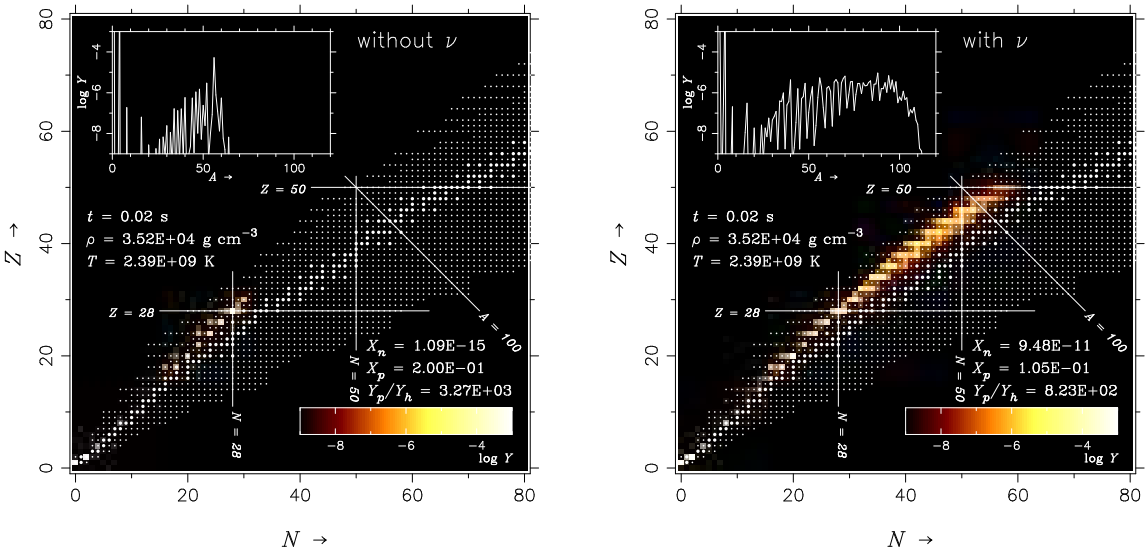

Figure 2: Snapshot of the nucleosynthesis at $t = 0.02$ s for the wind trajectory of $M = 2.0M_\odot$, $L_\nu = 4.0 \times 10^{51}$ ergs s^{-1}, $t_{\rm pb} = 2.0$ s, and $Y_{ei} = 0.600$, where the neutrino reactions are turned off (left panel) and on (right panel). The abundances are shown by the image in the nuclide chart. The abundance curve as a function of mass number is shown in the upper left for each panel.

Figure 2 shows the snapshot of nucleosynthesis at $t = 0.02$ s for the wind trajectory of $M = 2.0M_\odot$, $L_\nu = 4.0 \times 10^{51}$ ergs s^{-1}, $t_{\rm pb} = 2.0$ s, and $Y_{ei} = 0.600$, where the neutrino reactions are turned off (left panel) and on (right panel). Y_{ei} is the initial electron fraction (number of proton per baryon) at $T_9 = 9$ ($t = 0$ s). The entropy obtained for this trajectory is $129N_Ak$. Without neutrino reactions, the abundances have a sharp peak at ^{56}Ni and the nuclear flow stops at ^{64}Ge owing to its long half life (1.062 min) as well as the small proton-separation energies around these species. In contrast, the inclusion of neutrino reactions leads to the nuclear flow reaching the $Z = 50$ proton-magic number, resulting in the production of proton-rich isotopes beyond $A = 100$. This *neutrino-induced rp-process* is a consequence of the presence of neutrons formed by the capture of anti-electron neutrinos on free protons. As a result, the waiting point nuclei are bypassed via neutron captures (n, p) and (n, γ), and the proton capture proceeds.

The time evolution of Y_{ei} that determines the initial composition for each wind trajectory is assumed as in the top panel of Figure 3, so as to mimic the hydrodynamic results in [10]. Y_{ei} is taken to be constant (Y_{e0}) for $t_0 < t_{\rm pb} \le t_1$ and $Y_e(t_{\rm pb}) = (Y_{e0} - Y_{e1})(t_{\rm pb}/t_1)^{-1} + Y_{ef}$ for $t > t_1$, where $t_1 = 4.0$ s and $Y_{e1} = 0.100$. Y_{e0} is taken to be a free parameter, which varies from 0.460 to 0.630 with the interval of 0.005 (35 cases). It should be noted that Y_e changes during the α-process phase ($T_9 \sim 7-4$), affected by the neutrino capture on free nucleons. The bottom panel of Figure 3 shows

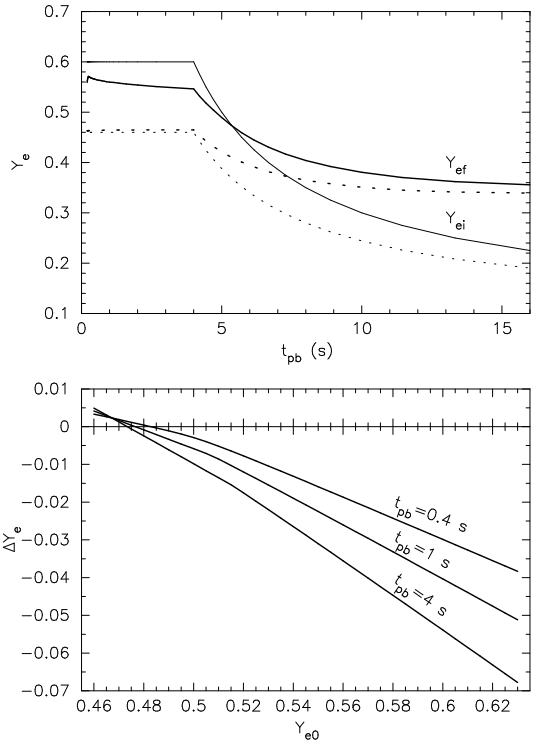

Figure 3: Top: time evolution of Y_{ei} (thin lines) and $Y_{ef} \equiv Y_{ei} + \Delta Y_e$ (thick lines) for $Y_{e0} = 0.600$ (solid lines) and 0.460 (dotted lines). Bottom: ΔY_e at $t_{\rm pb} = 0.4$, 1.0, and 4.0 s ($L_\nu = 20$, 8, and 2×10^{51} ergs s^{-1}, respectively), when the temperature decreases to $T_9 = 3$ (at which the *rp*-process sets in).

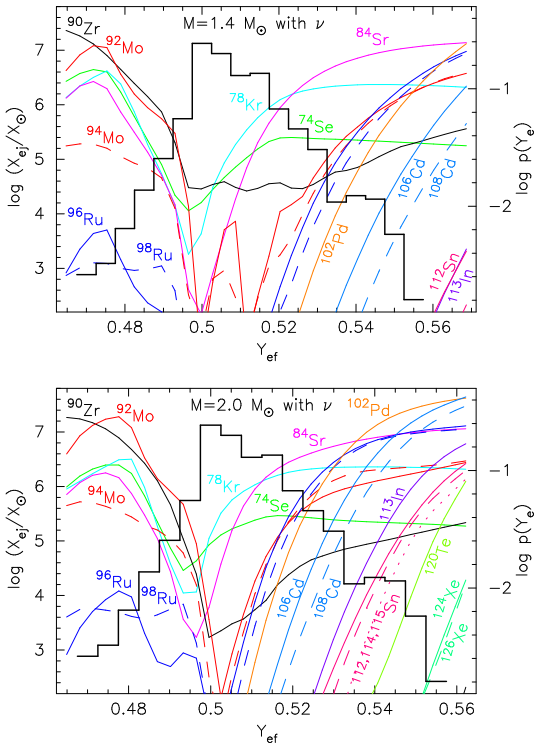

Figure 4: Top: mass-averaged abundances of *p*-nuclei (and ^{90}Zr for comparison purposes) with respect to their solar values for $M = 1.4 M_\odot$ case as functions of $Y_{ef}(t_{\rm pb} = 4.0$ s). Also shown is the histogram of the Y_e distribution $p(Y_e)$ of the neutrino-processed ejecta in a two-dimensional "exploding" core-collapse simulation by [3]. Bottom: same as the top panel, but for $M = 2.0 M_\odot$ case.

the shifts ΔY_e at $t_{\rm pb} = 0.4$, 1.0, and 4.0 s ($L_\nu = 20$, 8, and 2×10^{51} ergs s^{-1}, respectively), when the temperature decreases to $T_9 = 3$ (at which the *rp*-process sets in). The top panel shows Y_{ei} (thin lines) and $Y_{ef} \equiv Y_{ei} + \Delta Y_e$ (thick lines) for $Y_{e0} = 0.600$ (solid lines) and 0.460 (dotted lines).

4. CONTRIBUTION TO THE GALACTIC CHEMICAL EVOLUTION

In order to examine the contribution of this neutrino-induced *rp*-process to the Galactic chemical evolution, the yields for each Y_{ei} model (35 cases) are mass-averaged over the 54 wind trajectories weighted by $\dot{M}(L_\nu)\Delta t_{\rm pb}$. The mass-averaged abundances of *p*-nuclei with respect to their solar values for $M = 1.4 M_\odot$ (top) and $2.0 M_\odot$ (bottom) cases are shown in Figure 4, as functions of $Y_{ef}(t_{\rm pb} = 4.0$ s) (at $L_\nu = 2.0 \times 10^{51}$ ergs s^{-1}, as representative of different Y_{ef}s). Note that the production of *p*-nuclei during later phase ($t > 4.0$ s) are negligible owing to the neutron richness (Figure 3, top), where the neutron capture nucleosynthesis takes place. As can be seen, a variety of *p*-nuclei are produced with interesting amount for $Y_{ef} > 0.5$ models. The heavier *p*-nuclei (up to

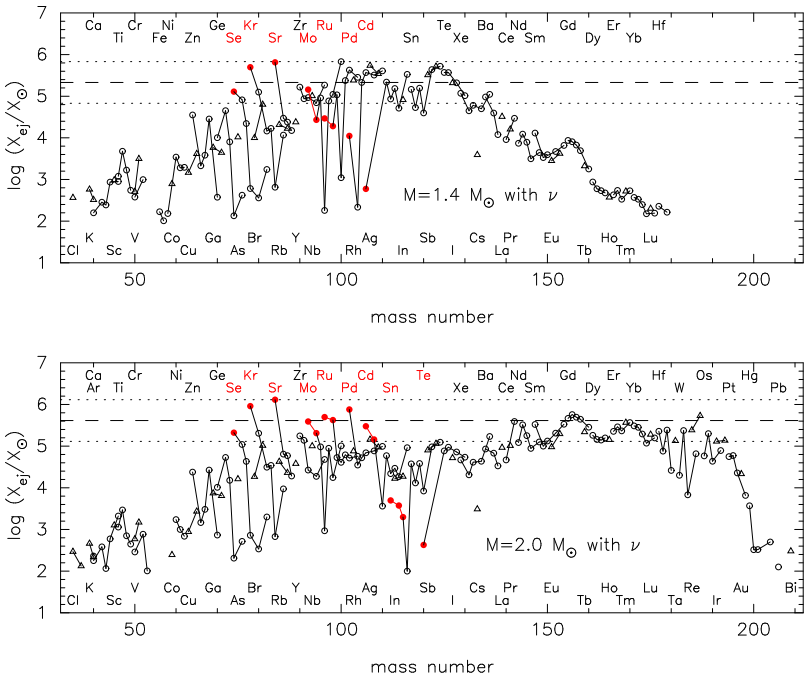

Figure 5: Mass-Y_e-averaged abundances with respect to their solar values for $M = 1.4M_\odot$ (top panel) and $2.0M_\odot$ (bottom panel) cases as functions of mass number. The isotopes (after decay) are denoted by circles (even-Z) and triangles (odd-Z). The p-nuclei are denoted with filled circles. The solid lines connect isotopes of a given element.

$A \approx 110-120$) appear for greater Y_{ef} models as well as for larger M ($= 2.0M_\odot$) case (i.e., greater entropies, see Figure 1). It should be noted that ^{74}Se and ^{92}Mo are most enhanced in slightly neutron-rich compositions (at $Y_{ef} \approx 0.48$, see [6, 12]).

In reality, the neutrino-heated matter must have a certain distribution of Y_e as can be seen in a two-dimensional hydrodynamic simulation of core-collapse supernova [3]. The Y_e distribution of the neutrino-processed ejecta during the first 468 ms after core bounce for a $15M_\odot$ progenitor star obtained by [3] is overlaid in Figure 4, which has the maximum at $Y_e \approx 0.5$ and dominates in the proton-rich side. To test the contributions of the winds for $M = 1.4M_\odot$ and $2.0M_\odot$ cases, the mass-averaged yields for each Y_{ei} model are further Y_e-averaged ($54 \times 35 = 1890$ winds in total) with $p(Y_e)$ shown in Figure 4, *assuming* this distribution to be representative of core-collapse supernovae. The resulting abundances with respect to their solar values are shown in Figure 5 for $M = 1.4M_\odot$ (top panel) and $2.0M_\odot$ (bottom panel) cases as functions of mass number. The p-nuclei are denoted with filled circles. The dotted horizontal lines indicate a "normalization band" between the largest production factor (^{84}Sr) and that by a factor of ten less than that, along with a median value (dashed line).

As can be seen in Figure 5, the p-nuclei up to ^{92}Mo and ^{108}Cd for $M = 1.4M_\odot$ and $2.0M_\odot$ cases, respectively, fall within the normalization band, which are regarded to be the dominant species produced by each event. Note that ^{74}Se and ^{92}Mo are mainly from the slightly neutron-rich ejecta as described above, while other p-nuclei are synthesized by the neutrino-induced *rp*-process

in the proton-rich ejecta. The ejected masses by winds during the first 20 s are $2.8 \times 10^{-3} M_\odot$ and $1.1 \times 10^{-3} M_\odot$ for $M = 1.4 M_\odot$ and $2.0 M_\odot$ cases, respectively. Given that the progenitor mass for each case to be, e.g., $15 M_\odot$ and $30 M_\odot$, respectively, the overproduction factor is expressed as $\sim 10^{-4} (X_{\rm ej}/X_\odot)$. The requisite overproduction factor of a given isotope for the nucleosynthetic event to be the major source in the solar system is ~ 10 [10], assuming that *all* the core-collapse supernovae produce the same amount of the isotope. The overproduction factors of $\sim 10 - 100$ (see Figure 5) for the current models imply that the neutrino-driven winds can be potentially the major astrophysical site of these light *p*-nuclei.

The neutron-capture nuclei with $A > 100$ result from winds during the later phase ($t_{\rm pb} > 4.0$ s, see Figure 3, top panel), where the initial compositions are presumed to be neutron rich. In fact, the high-entropy winds of $M = 2.0 M_\odot$ case are those proposed to be the astrophysical origin of the heavy *r*-process nuclei [7, 13], while that of $M = 1.4 M_\odot$ to be the origin of light *r*-process nuclei up to $A \sim 130$ [13]. It is interesting to note that no overproduction of the $A \approx 90$ nuclei [7, 10] appears owing to the neutron deficiency in the ejecta [13].

5. SUMMARY

It is shown that the interesting amounts of *p*-nuclei can be produced by the neutrino-induced *rp*-process in the proton-rich neutrino-driven winds of core-collapse supernovae. This is due to the presence of free neutrons by the anti-electron neutrino capture on free protons, which bypass the known waiting point nuclei along the nuclear path of the *rp*-process. The nucleosynthesis calculations imply that this neutrino-induced *rp*-process in core-collapse supernovae can be potentially the origin of light *p*-nuclei up to $A \sim 110$, which cannot be easily explained by other astrophysical scenarios.

References

[1] R. K. Wallace and S. E. Woosley, *Astrophys. J.* **45**, 389 (1981).

[2] O. Koike, M. Hashimoto, K. Arai, and S. Wanajo, *Astron. Astrophys.*, **342**, 464 (1999).

[3] R. Buras, M. Rampp, H. -Th Janka, and K. Kifonidis, *Astron. Astrophys.*, **447**, 1049 (2006).

[4] J. Pruet, R. D. Hoffman, S. E. Woosley, H. -Th. Janka, and R. Buras, *Astrophys. J.*, **644**, 1028 (2006).

[5] C. Fröhlich, et al. *Astrophys. J.*, **637**, 415 (2006).

[6] S. Wanajo, *Astrophys. J.*, **647**, 1323 (2006).

[7] S. Wanajo, T. Kajino, G. J. Mathews, and K. Otsuki, *Astrophys. J.*, **554**, 578 (2001).

[8] S. Wanajo, N. Itoh, Y. Ishimaru, S. Nozawa, and T. C. Beers, *Astrophys. J.*, **577**, 853 (2002).

[9] S. Wanajo, *Astrophys. J.*, **650**, L79 (2006).

[10] S. E. Woosley, J. R. Wilson, G. J. Mathews, R. D. Hoffman, and B. S. Meyer, *Astrophys. J.*, **433**, 229 (1994).

[11] S. Wanajo, S. Goriely, M. Samyn, and N. Itoh, Y., *Astrophys. J.*, **606**, 1057 (2004).

[12] R. D. Hoffman, S. E. Woosley, G. M. Fuller, and B. S. Meyer, *Astrophys. J.*, **460**, 478 (1996).

[13] S. Wanajo and I. Ishimaru, *Nucl. Phys. A*, **777**, 676 (2006).